BJP British Journal of Pharmacology

DOI:10.1111/bph.12482
www.brjpharmacol.org

RESEARCH PAPER

Constitutive activation of AMPK α1 in vascular endothelium promotes high-fat diet-induced fatty liver injury: role of COX-2 induction

Yan Liang, Bosheng Huang, Erfei Song, Bo Bai and Yu Wang

Department of Pharmacology and Pharmacy, LKS Faculty of Medicine, The University of Hong Kong, Hong Kong, China

Correspondence
Dr Yu Wang, Department of Pharmacology and Pharmacy, The University of Hong Kong, 21 Sassoon Road, Pokfulam, Hong Kong, China. E-mail: yuwanghk@hku.hk

Keywords
AMPK; endothelial cells; fatty liver injury; cyclooxygenase-2

Received
26 May 2013
Revised
24 September 2013
Accepted
16 October 2013

BACKGROUND AND PURPOSE

AMP-activated protein kinase (AMPK), an important regulator of energy metabolism, comprises three (α, β and γ) subunits, each with a unique tissue distribution. As AMPK has a wide range of protein and gene targets, defining its role has been difficult. Here, we have studied a transgenic mouse model overexpressing the constitutively active α1 subunit of AMPK in endothelial cells (EC-AMPK) to elucidate its role in energy homeostasis.

EXPERIMENTAL APPROACH

Wild-type and EC-AMPK mice were fed with a high fat diet for 16 weeks. Drugs (or vehicles) were given daily by oral gavage. Body weight, fat mass composition, glucose and lipid levels were monitored regularly. Tissues including aortae and liver were collected for quantitative RT-PCR, Western blotting, ELISA, histological and biochemical evaluations.

KEY RESULTS

Compared with wild-type animals, high fat diet caused more severe metabolic defects in EC-AMPK mice, which exhibited increased body weight and fat mass, elevated blood pressure, augmented glucose and lipid levels, impaired glucose tolerance, hepatomegaly and steatohepatitis. Constitutive activation of AMPK α1 in endothelial cells induced COX-2 expression and arterial inflammation. Genes involved in lipid metabolism were down-regulated in aortae and livers of EC-AMPK mice. Chronic treatment with selective COX-2 inhibitors, celecoxib or nimesulide, significantly ameliorated arterial inflammation, steatohepatitis and hyperlipidaemia in EC-AMPK mice, without altering their blood pressure or clotting.

CONCLUSIONS AND IMPLICATIONS

Constitutive activation of endothelial AMPK α1 promotes vascular inflammation and the development of obesity-induced fatty livers largely via induction of COX-2.

Abbreviations

ALT, alanine aminotransferase; AMPK, 5′-adenosine monophosphate-activated protein kinase; AST, aspartate aminotransferase; CA-AMPK, constitutively active AMPK; CD68, cluster of differentiation 68; EC-AMPK, transgenic mice with endothelial-selective overexpression of CA-AMPK α1 subunit; EL, endothelial lipase; ICAM-1, intercellular adhesion molecule-1; ipGTT, intraperitoneal glucose tolerance tests; LDLR, low-density lipoprotein receptor; NPC, non-parenchymal cells;

© 2013 The British Pharmacological Society

Introduction

5′-Adenosine monophosphate-activated protein kinase (AMPK), an evolutionarily conserved serine/threonine kinase, plays a central role in maintaining energy homeostasis (Hardie *et al.*, 2012). AMPK functions by phosphorylation of key metabolic enzymes, switching off biosynthetic pathways and switching on catabolic pathways. It also exerts regulatory effects on gene expression and protein synthesis (Hardie, 2011). AMPK has been considered as a potential drug target for the treatment of cardiometabolic abnormalities associated with obesity and type 2 diabetes. It is activated by metformin, the most commonly used anti-diabetic drug (Davis *et al.*, 2006), and by salicylate, the breakdown product of aspirin (Hawley *et al.*, 2012).

Functional AMPK is a trimeric complex comprising one catalytic α subunit and one each of the non-catalytic β and γ subunits (Carling *et al.*, 2012). Phosphorylation of the conserved threonine residue (Thr^{172}) within the α subunit stimulates the activation of AMPK (Woods *et al.*, 2003), which is enhanced by AMP binding to the γ subunit (Chen *et al.*, 2009). The catalytic activity of AMPK α subunit is inhibited by its auto-inhibitory domain (Stein *et al.*, 2000). A truncated α subunit containing only the kinase domain exhibits full activity in the absence of AMP binding. When Thr^{172} is replaced by aspartic acid (T172D), this truncated α subunit acts as a constitutively active form of AMPK (CA-AMPK) (Stein *et al.*, 2000).

In blood vessels, AMPK triggers vasodilatation and participates in blood flow regulation. Activation of AMPK represents an additional mechanism by which physiological and pathological stresses, such as exercise, inflammation, hypoxia and ischaemia, induce the dilation of large arteries (Ewart and Kennedy, 2011). However, both AMPK α1 and AMPK α2 knockout mice are able to produce vasodilatation in response to ACh stimulation. Thus, the overall contribution of AMPK activation in endothelial NO formation is disputed (Fisslthaler and Fleming, 2009). In fact, pharmacological activators of AMPK mainly act on the smooth muscle cells to promote vascular relaxation (Goirand *et al.*, 2007; Chang *et al.*, 2010).

In endothelial cells, the AMPK α1 subunit, but not the α2 subunit, is predominantly expressed (Ewart and Kennedy, 2011). While the α2 subunit is critical in maintaining the non-atherogenic phenotype of endothelial cells (Wang *et al.*, 2010), the α1 subunit in the endothelium plays a pro-survival and anti-apoptotic role, which involves the activation of pro-inflammatory NF-κB signalling (Liu *et al.*, 2010). The present study demonstrated that in a transgenic mouse model with selective overexpression of CA-AMPK α1 subunit in endothelial cells (EC-AMPK), high fat diet induced more severe hepatomegaly and steatohepatitis, which could be attenuated by chronic treatment with selective COX-2 inhibitors.

Methods

Animals and drug treatment

All animal care and experimental procedures were approved by the Institutional Committee on the Use of Live Animals in Teaching and Research of the University of Hong Kong (CULATR No. 2282-10). All studies involving animals are reported in accordance with the ARRIVE guidelines for reporting experiments involving animals (Kilkenny *et al.*, 2010; McGrath *et al.*, 2010). A total of 72 male mice were used in the experiments described here. EC-AMPK mice were cross-bred with C57BL/6J wild-type mice for more than 12 generations (Li *et al.*, 2012). PCR genotyping was performed to select transgenic mice using forward (5′-GGGGATATGACACCTGC-3′) and reverse (5β-CGTCGTGCTTCTGCTT-3′) primers. The wild-type littermates were included as experimental controls. All animals were maintained in a temperature-controlled facility under 12 h light–dark cycles and with free access to water and chow. Starting from the age of 4 weeks, animals were supplied with a high fat diet (D12451; Research Diet, New Brunswick, NJ, USA) for another 16 weeks. Body weight, food intake, fat mass composition and blood glucose levels were monitored once every 2 weeks (Law *et al.*, 2010). Drug treatment was performed during the last 4 weeks of high-fat diet feeding. Briefly, mice were randomly divided into two subgroups for oral administration of vehicle (0.3% methyl cellulose) or one of the selective COX-2 inhibitors, celecoxib (25–50 $mg \cdot kg^{-1} \cdot day^{-1}$; Selleck Chemicals, Munich, Germany) or nimesulide (25 $mg \cdot kg^{-1} \cdot day^{-1}$; Sigma-Aldrich, St. Louis, USA). Unless specified, the comparisons were between mice fed with high fat diet.

Metabolic evaluation

Intraperitoneal glucose tolerance test (ipGTT) was performed using mice that were fasted overnight as described (Law *et al.*, 2010). Body composition of unanaesthetized mice was assessed by NMR using a Brucker Minispec Live Mice Analyzer (model mq7.5, LF50; Bruker Optics, Inc., Billerica, MA, USA). At the end of treatment, mice were killed under deep anaesthesia with hypnorm/dormicum (fentanyl 0.4 $mg \cdot kg^{-1}$, fluanisone 12.5 $mg \cdot kg^{-1}$, dormicum 6.25 $mg \cdot kg^{-1}$, i.p., Roche). Serum samples were collected from the saphenous vein of mice after 16 h of fasting. Individual kits were purchased from Stanbio Laboratory (Boerne, TX, USA) for measuring serum concentrations of triglyceride, cholesterol, high- (HDL) and low-density lipoprotein cholesterols (LDL), alanine aminotransferase (ALT) and aspartate aminotransferase (AST). The content of hepatic triglyceride was determined using tissue lipids extracted by the Folch method with slight modifications (Zhou *et al.*, 2010).

Blood pressure measurements

Arterial blood pressure was measured with an automated tail-cuff BP-2000 Blood Pressure Analysis System (Visitech Systems, Apex, NC, USA) as described (Liu *et al.*, 2012). The systolic and diastolic blood pressure were recorded and averaged from at least 10 consecutive readings.

Tail bleeding

The bleeding time protocol was adapted from methods described previously (Henry *et al.*, 2009). In brief, mice were immobilized and tails were clipped 2 mm from the tip and immediately immersed into 37°C saline. The time to bleeding cessation was recorded by measuring the OD (405 nm) of

samples mixing with the red blood cell lysis buffer. The volume of blood loss was calculated for comparison.

Liver cell fractionation

Liver perfusion was performed as described (Zhou *et al.*, 2012). After removing tissue aggregates and debris, cell suspensions were filtered through a strainer (mesh width 100 μm). Parenchymal and non-parenchymal cells (NPCs) were fractionated by low-speed centrifugation.

AMPK activity assay

Tissues were homogenized in lysis buffer [20 mM Tris–HCl, pH 7.5, 150 mM NaCl, 1 mM Na_2EDTA, 1 mM EGTA, 1% Nonidet P40, 0.1% SDS, 1% sodium deoxycholate, 1 mM NaF, 1 mM Na_3VO_4, 1 mM DTT and protease inhibitor cocktails (Roche, Mannheim, Germany)]. The tissue lysates (15 μg) were re-suspended in assay buffer of CycLex AMPK kinase kit (MBL International, Woburn, MA, USA) and incubated with the IRS-1 peptide (LRLSSSSGRLR) substrate at 30°C for 30 min. Phosphorylation of the Ser^{789} was quantified with a specific antibody for evaluating the activity of AMPK in tissue samples.

Histological studies

Paraffin sections (5 μm) of liver tissues were stained with haematoxylin and eosin. Images were acquired under a microscope (Leica Microsystems, Bensheim, Germany). Inflammatory foci (defined as groups of five or more inflammatory cells) were counted in at least 10 fields, each representing about 300 hepatocytes. Inflammation status was graded as follows: grade 0, no inflammatory foci; grade 1, one inflammatory foci per high powered field (hpf); grade 2, two inflammatory foci per hpf; grade 3, three or more inflammatory foci per hpf (Zhou *et al.*, 2010).

Quantitative RT-PCR analysis

Quantification of gene expression was performed using SYBR Green PCR Master Mix (Qiagen, Hamburg, Germany) and an ABI PRISM 7900 HT Sequence Detection System (Life Technologies, Grand Island, NY, USA). The primer sequences are listed in Supporting Information Table S1. After normalization, data were calculated and presented as relative expression changes of the transcripts.

COX-2 activity assay

The COX-2 activity was evaluated in tissue lysates by measuring the stable metabolite of prostacyclin, 6-keto-prostaglandin $F_{1\alpha}$ ($PGF_{1\alpha}$), using the commercial EIA Kit (Cayman, Ann Arbor, MI, USA). The assay was performed based on the competition between 6-keto-$PGF_{1\alpha}$ and a tracer for the anti-serum binding sites. In brief, aortae or liver tissues were homogenized in lysis buffer included in the kit. After incubation, the amount of tracer bound to the plate was quantified by enzymatic colour reaction and measured at 412 nm. The amount of 6-keto-$PGF_{1\alpha}$ was calculated by referring to the standard curves.

Western blotting and other immunoassays

Tissue lysates were separated by SDS-PAGE and transferred to polyvinylidene difluoride membrane, incubated with antibodies against COX-2 and β-actin (Cell Signaling, Beverly, MA, USA). The immune complexes were detected with enhanced chemiluminescence reagents from GE Healthcare (Uppsala, Sweden). The tissue contents of TNF-α were measured using commercial ELISA kits (Invitrogen, Grand Island, NY, USA). TxB_2, the stable metabolite of the COX product TxA_2, was measured with the TxB_2 EIA Kit from Cayman.

Data analysis

All the results were derived from at least three independent experiments. Values are expressed as means ± SEM. The statistical calculations were performed by one-way ANOVA followed by Tukey's multiple comparisons using Prism version 5 (GraphPad Software, San Diego, CA, USA). For all comparisons, a $P < 0.05$ was accepted to indicate statistically significant differences.

Results

Severe hepatomegaly and steatohepatitis in EC-AMPK mice maintained on a high fat diet

With standard chow, the body weight, fat mass composition, fasting blood glucose and lipid levels were similar between wild-type and EC-AMPK mice (Table 1). After 16 weeks of the high fat diet, the body weight and percentage fat mass of EC-AMPK mice were increased by ~1.8- and ~2.2-fold respectively. The gain of body weight and fat mass, fasting blood glucose levels, serum concentrations of triglyceride, total cholesterol, HDL and LDL cholesterol, as well as systolic BP of EC-AMPK mice were all augmented by the high fat diet, to levels significantly greater than those of wild-type mice (Table 1). Glucose tolerance was further impaired in EC-AMPK mice, as revealed by the ipGTT (Supporting Information Figure S1).

In EC-AMPK mice, the liver to body weight ratios and hepatic triglyceride contents were significantly higher (by 23 and 57%, respectively) than those of wild-type mice (Figure 1A). Histological analysis revealed a much wider range of large and small lipid droplet accumulation, and a higher grade of inflammation in liver sections of EC-AMPK mice than those of wild-type mice (Figure 1B). More severe liver injury in EC-AMPK mice was further confirmed by biochemical measurement of serum ALT and AST levels (Figure 1C), and by quantitative RT-PCR gene expression analysis of the inflammatory markers F4/80 and CD68 (Figure 1D).

Thus, the high fat diet induced a more severe metabolic syndrome in EC-AMPK mice, which was manifested in liver as the characteristic phenotypes of enlargement (hepatomegaly), lipid accumulation (steatosis) and inflammation (hepatitis).

Overexpression of AMPK α1 subunit promoted inflammation and COX-2 expression in arteries of EC-AMPK mice

The expression of the CA-AMPK α1 transgene was confirmed in aortae of EC-AMPK mice by both RT-PCR and Western blotting analysis (Figure 2A). As expected, a 36 kDa protein

Table 1

Metabolic parameters measured in 20-week-old wild-type and EC-AMPK mice fed with either standard chow (STD) or high fat diet (HFD)

	Wild type (STD)	Wild type (HFD)	EC-AMPK (STD)	EC-AMPK (HFD)
Body weight (g)	26.9 ± 1.28	44.9 ± 1.69	27.1 ± 0.80	50.1 ± 1.04*
Fat mass (%)	13.7 ± 0.30	26.7 ± 1.44	13.9 ± 0.64	31 ± 0.90*
Lean mass (%)	70 ± 1.11	53 ± 1.46	69.5 ± 0.67	48.8 ± 1.14*
Fasting glucose (mmol·L^{-1})	4.4 ± 0.47	7.8 ± 0.81	4.5 ± 0.56	9.4 ± 0.85*
Triglyceride (mg·L^{-1})	385 ± 54	621 ± 51.7	440 ± 55.7	935 ± 48.1*
Total cholesterol (mg·L^{-1})	578 ± 11.6	1360 ± 147	571 ± 29.9	1990 ± 122*
High-density lipoprotein cholesterol (mg·L^{-1})	287 ± 25.9	618 ± 54.7	335 ± 29.7	1254 ± 67.2*
Low-density lipoprotein cholesterol (mg·L^{-1})	549 ± 44	854 ± 89.5	609 ± 38.8	2121 ± 92.3*
Systolic blood pressure (mmHg)	101 ± 5.8	106 ± 6.3	101 ± 5.9	124 ± 7.0*

*P < 0.05, EC-AMPK (HFD) versus wild-type (HFD) group, n = 8–10.

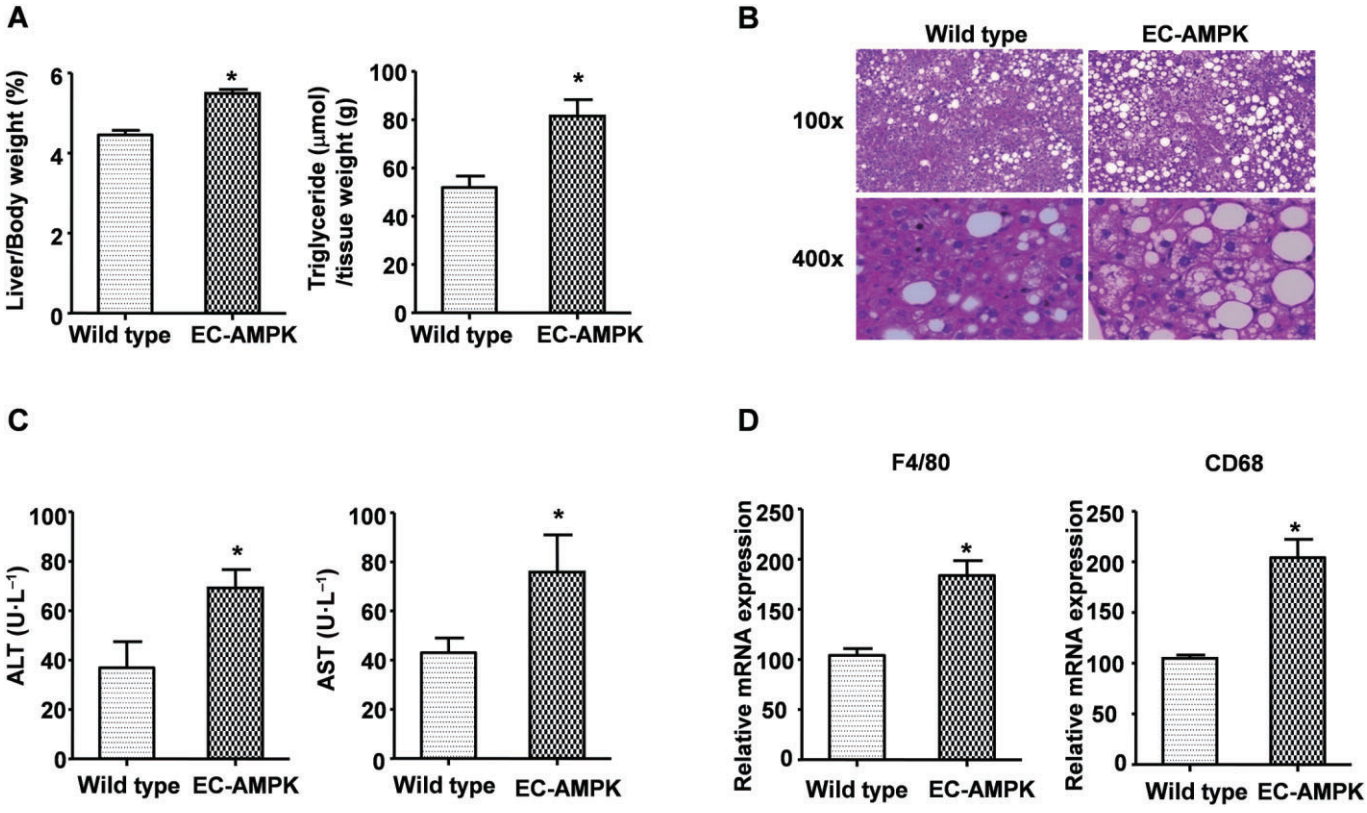

Figure 1

Hepatomegaly and severe steatohepatitis in EC-AMPK mice fed with high-fat diet. After 16 weeks of high fat diet, liver tissues were collected from wild-type and EC-AMPK mice for measuring the wet weights and triglyceride contents (A), and histological analysis after haematoxylin and eosin staining (B). Magnification: 100× and 400×. Serum levels of alanine aminotransferase (ALT) and aspartate aminotransferase (AST) were quantified by commercial assay kits (C). The mRNA expression of inflammatory markers F4/80 and CD68 was evaluated by quantitative RT-PCR analysis and calculated as percentage changes against samples derived from wild-type mice (D). *P < 0.05 versus wild type mice group, n = 5–8.

band corresponding to CA-AMPK α1 subunit was present in the aortae of EC-AMPK mice, but not in that of wild-type mice (Li *et al.*, 2012). The mRNA and protein expression of the transgene could not be detected in total tissue lysates of EC-AMPK mice livers (Figure 2A). However, the mRNA expression of CA-AMPK was revealed by RT-PCR in isolated NPCs (Supporting Information Figure S2). AMPK activity in the aortae of EC-AMPK mice was elevated by 2.7-fold when compared to that of wild-type mice (Figure 2B). In livers of EC-AMPK mice, the basal AMPK activity was increased by

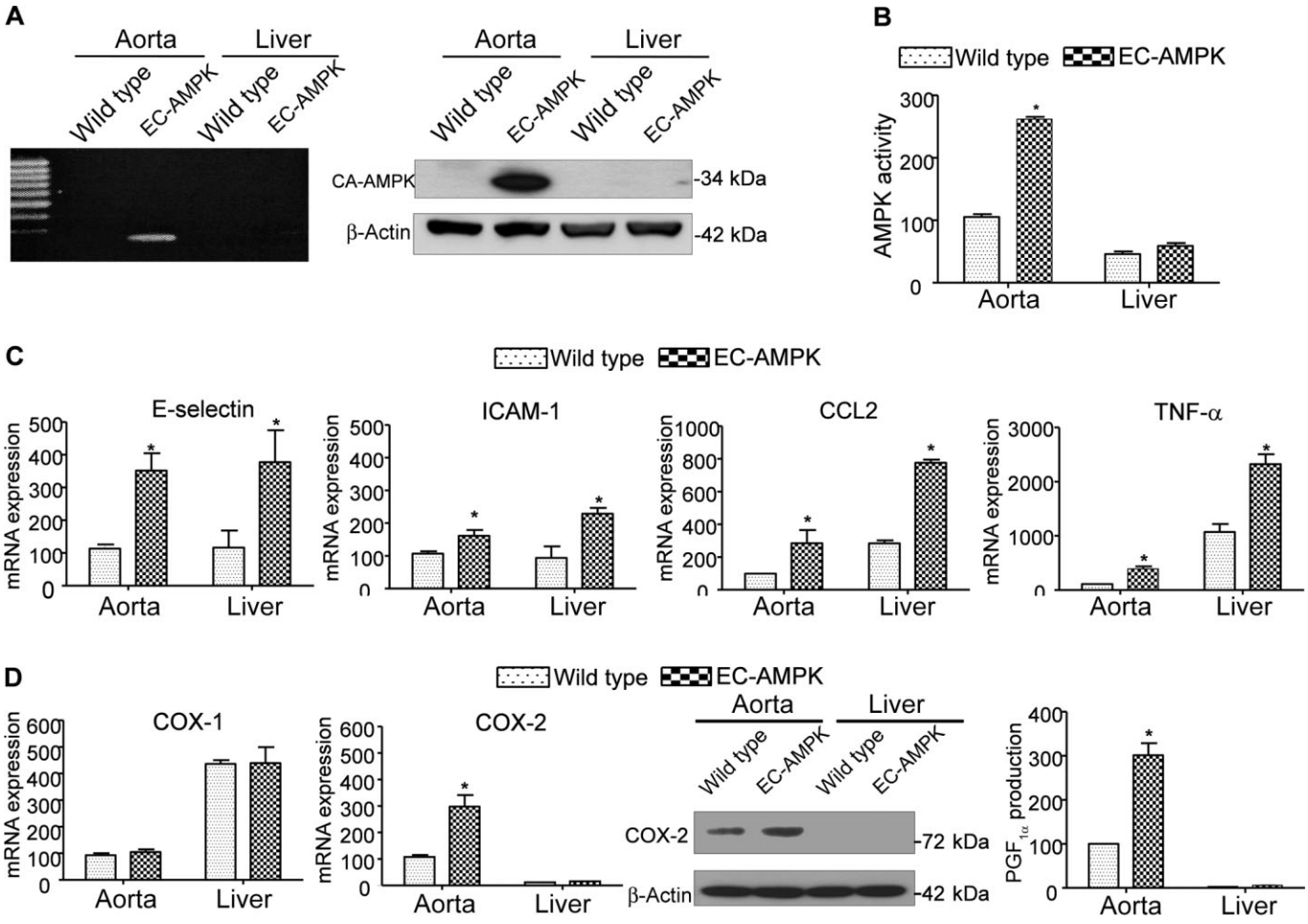

Figure 2

Enhanced arterial and hepatic inflammation in EC-AMPK mice given a high fat diet. Aortae and liver tissues were collected from wild- type and EC-AMPK mice as in Figure 1. The expression of CA-AMPK transgene was confirmed by RT-PCR and Western blotting (A). AMPK activity was measured by biochemical assay as described in the Methods section (B). Quantitative RT-PCR was performed to compare the gene expression of inflammatory markers, including E-selectin, ICAM-1, CCL2 and TNF-α in aortae and liver (C). The expression (both mRNA and protein) and activity of COX-2 was measured and compared between wild-type and EC-AMPK mice by quantitative RT-PCR, Western blotting and ELISA of the metabolite PGF1α respectively (D). All results were calculated and presented as percentage changes against the values of samples derived from aortae of wild-type mice. *$P < 0.05$ versus wild-type mice, $n = 3–5$.

1.5-fold (Figure 2B), due mainly to the augmented AMPK activity in non-parenchymal liver cells (Supporting Information Figure S2).

Quantitative RT-PCR analysis revealed that the expression of inflammation-related genes, including E-selectin, intercellular adhesion molecule-1 (ICAM-1), the chemokine CCL2 and TNF-α, were all significantly up-regulated in the aortae of EC-AMPK mice when compared to those of wild-type mice (Figure 2C). While the expression of these genes was similarly elevated in the liver tissues of EC-AMPK mice (Figure 2C), the expression of COX-2 was significantly augmented in the aortae of EC-AMPK mice (Figure 2D). The mRNA levels of COX-1 were not different between wild-type and EC-AMPK mice. Up-regulated COX-2 expression and activity were further confirmed by Western blotting and immunoassay measurement of its metabolite, $PGF_{1\alpha}$. Compared with that of aortae, the expression of COX-2 was barely detectable by Western blotting in liver tissues of both groups of mice. The expression of endothelial lipase (EL) and LDL receptor (LDLR), two important regulators of lipoprotein cholesterol metabolism, was significantly decreased in the aorta and liver tissues of EC-AMPK mice (Supporting Information Figure S3).

The above results suggested that constitutive activation of AMPK α1 in endothelial cells caused not only hepatic inflammation but also vascular inflammation accompanied by abnormal expression of key regulators of cholesterol metabolism.

Chronic treatment with selective COX-2 inhibitors alleviated aortic inflammation and steatohepatitis in EC-AMPK mice

COX-2 expression is normally absent from most tissues. Once being induced to express, it acts as a major inflammatory mediator. To evaluate whether increased COX-2 expression

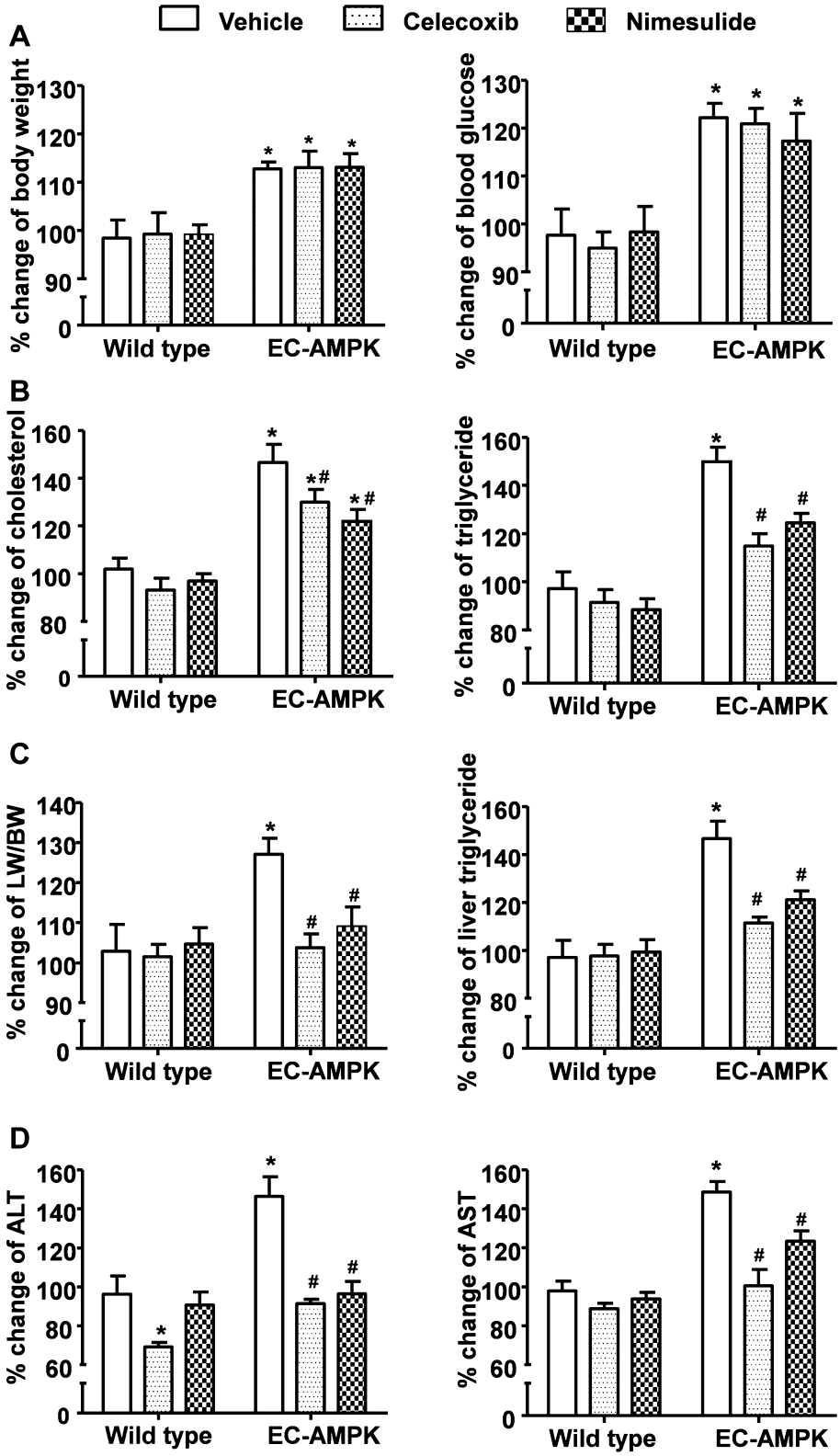

Figure 3

Reduced hepatic lipid contents and alleviated liver injury in EC-AMPK mice treated with selective COX-2 inhibitors. Wild-type and EC-AMPK mice given a high fat diet were treated with vehicle, celecoxib or nimesulide for a period of 4 weeks. At the end of treatment, parameters including body weight and circulating glucose (A), serum triglyceride and cholesterol levels (B), liver to body weight ratios (LW/BW) and hepatic triglyceride contents (C), as well as serum levels of ALT and AST (D) were measured and presented as percentage comparisons against those from vehicle-treated wild-type mice. *$P < 0.05$ versus wild-type mice treated with vehicle; #$P < 0.05$ versus EC-AMPK mice treated with vehicle, $n = 3–5$.

contributed to the systemic inflammation of EC-AMPK mice, selective inhibitors of this enzyme, celecoxib and nimesulide, were chronically administered to mice during the last 4 weeks of high-fat diet feeding. The treatment with either drug had no effects on body weight and blood glucose levels (Figure 3A), but significantly decreased the circulating triglyceride and cholesterol levels in EC-AMPK mice (Figure 3B). Moreover, these drugs reduced the hepatomegaly, hepatic triglyceride contents, and serum ALT and AST levels in EC-AMPK mice (Figure 3C,D). After treatment, the $PGF_{1\alpha}$ was significantly decreased in the aortae of EC-AMPK mice (Figure 4A), whereas the AMPK activity was not altered (Supporting Information Figure S4A). In liver, while the concentration of $PGF_{1\alpha}$ was 10–20-fold lower than that of the aortae, treatment with both drugs was able to further decrease the production of this lipid metabolite. In addition, celecoxib or nimesulide significantly blunted the elevated production of TNF-α and CCL2 in both aortae and liver tissues of EC-AMPK mice, but had no obvious effects in wild-type mice (Figure 4C). The expression of EL and LDLR in livers of EC-AMPK mice was significantly up-regulated after treatment with both COX-2 inhibitors, whereas the expression of EL in aortae was not increased (Figure 5). BPs were not affected by treatment with celecoxib at different dosages (Supporting Information Figure S5A). Although celecoxib and nimesulide may also act on COX-1, blood clotting and TxB_2 concentrations were not significantly different before and after drug treatment in all experimental groups (Supporting Information Figure S5B, C).

These data indicated that selective inhibition of COX-2 eliminated most of the metabolic defects and inflammatory responses caused by constitutive activation of AMPK α1 in endothelial cells of EC-AMPK mice. There were no toxic effects observed due to COX-1 inhibition.

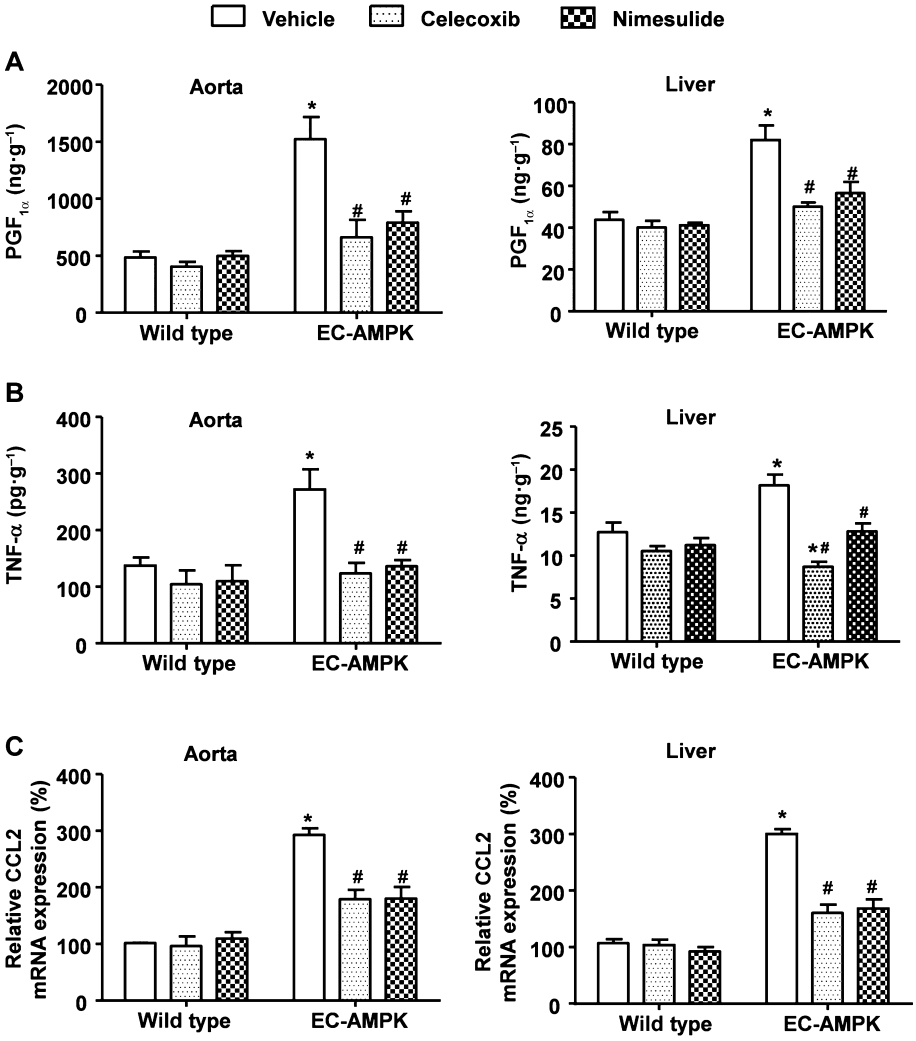

Figure 4

Celecoxib or nimesulide treatment inhibited arterial and hepatic inflammation in EC-AMPK mice given a high fat diet. Tissues were collected from wild-type and EC-AMPK mice treated as in Figure 3 and PGF1α concentrations measured (A), TNF-α contents (B) and CCL2 mRNA expression (C). Relative comparisons were calculated against samples from wild-type mice treated with vehicle. *$P < 0.05$ versus wild-type mice treated with vehicle; #$P < 0.05$ versus EC-AMPK treated with vehicle, $n = 3–5$.

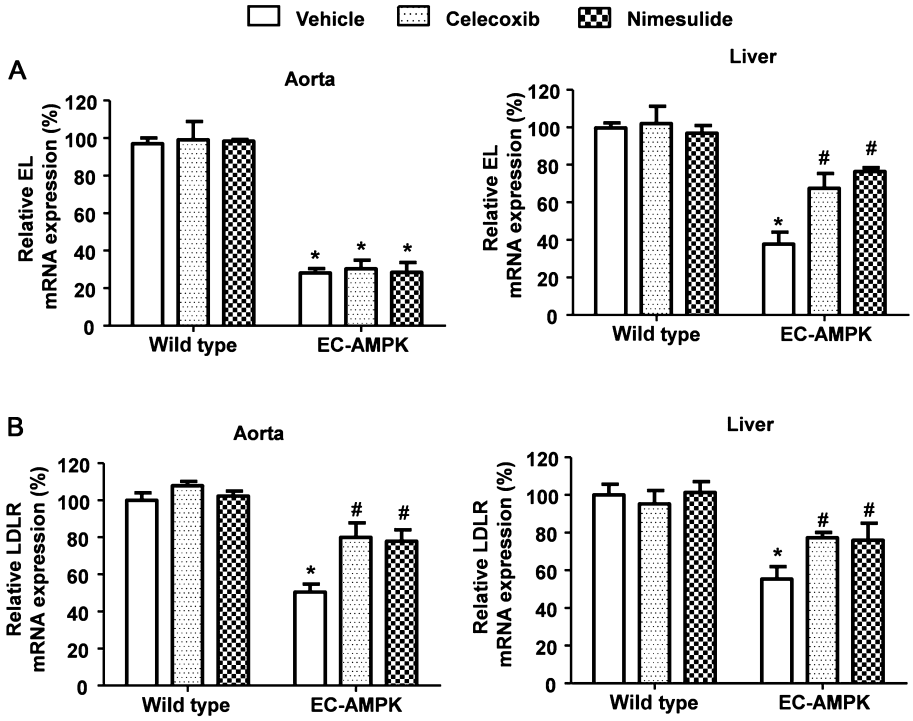

Figure 5

Treatment with celecoxib or nimesulide restored the gene expression of EL and LDLR in liver tissues of EC-AMPK mice. Tissues were collected from wild-type and EC-AMPK mice treated as in Figure 3 for quantitative RT-PCR analysis of EL (A) and LDLR (B) mRNA expressions. Relative comparisons were calculated against samples from wild-type mice treated with vehicle. *$P < 0.05$ versus wild-type mice treated with vehicle; #$P < 0.05$ versus EC-AMPK treated with vehicle, $n = 3–5$.

Discussion

Many pathological conditions of the cardiometabolic system, such as myocardial infarction, hypertension and diabetes, are associated with increased cellular stresses that can activate AMPK (Ewart and Kennedy, 2011). While the majority of studies have focused on the energy sensing and the beneficial metabolic effects of AMPK, there is considerable evidence suggesting a close relationship between AMPK activation and COX-2 induction. AMPK regulates COX-2 expression through stimulating the production of intracellular NO and mitochondrial reactive oxygen species, promoting the cytoplasmic localization of the human antigen R, and the activation of NF-κB, TGFβ-activated protein kinase 1 and PKCθ signalling (Faour *et al.*, 2008; Hou *et al.*, 2008; Zhang and Bowden, 2008; Chang *et al.*, 2010; Kim *et al.*, 2012; Lee *et al.*, 2012). Long-term AMPK activation also alters gene expression and protein synthesis by modulation of transcription factors, such as myocyte enhancer factor-2, mammalian target of rapamycin and eukaryotic elongation factor 2 (Kahn *et al.*, 2005). Increased expression of COX-2 would represent a pro-inflammatory function that may offset some protective effects of AMPK activation. The present study demonstrated that constitutive activation of AMPK α1 subunit in endothelial cells of arteries resulted in vascular inflammation and COX-2 induction, in turn, promoting the metabolic syndrome and fatty liver injury induced by a high fat diet.

COX-2 is expressed at low levels in resting endothelial cells and can be markedly induced by shear stress, reactive oxygen intermediates and fatty acid derivatives (Feng *et al.*, 1995; Eligini *et al.*, 2001; 2005; Di Francesco *et al.*, 2009; Brkic *et al.*, 2012). The activation of COX-2 plays a healing role in promoting vasodilation (through prostacyclin) and endothelial repair (Eligini *et al.*, 2009; Cannon and Cannon, 2012; Li *et al.*, 2012). It modulates endothelial NO production, platelet aggregation and the local inflammatory response during the development of atherosclerosis and thrombosis (Sanchez *et al.*, 2010; Santilli *et al.*, 2012; Yu *et al.*, 2012). High levels of COX-2 expression have been found in coronary arterioles of diabetic patients (Szerafin *et al.*, 2006; Tong *et al.*, 2013). In addition, increased COX-2 expression is correlated with obesity-related renal damage (Dey *et al.*, 2004), cardiac abnormalities (Cao *et al.*, 2011) and fatty liver injuries (Hsieh *et al.*, 2009). The expression levels of COX-2 are extremely low in normal liver tissues, but up-regulated under pathological conditions such as acute liver failure (Demirel *et al.*, 2012), hepatic fibrosis and cirrhosis (Kwon *et al.*, 2012), as well as hepatocarcinogenesis (Giannitrapani *et al.*, 2009). Genetic polymorphism of COX-2 has been linked with liver disease progression in human (Miyashita *et al.*, 2012). Both clinical and animal studies demonstrate that selective inhibition of COX-2 attenuates liver dysfunctions associated with hepatic inflammation, fibrosis, cirrhosis and cancer (Planaguma *et al.*, 2005; Breinig *et al.*, 2007; Tu *et al.*, 2007; Hsieh *et al.*, 2009; Paik *et al.*, 2009). In the present study, blocking COX-2 activ-

ity with the selective inhibitors, celecoxib or nimesulide, alleviated hepatic inflammation and steatosis in EC-AMPK mice. Treatment with these two drugs also reduced circulating lipid levels and inhibited arterial inflammation. The drug applications did not affect AMPK activity, suggesting that this kinase is an upstream signal of COX-2 activation in vascular endothelium and this pathway may represent a pro-inflammatory arm of AMPK function.

AMPK exists as a heterotrimeric complex composed of different subunits. The isoform abundance of each subunit varies in different types of cells and even in different arteries. Thus, when AMPK is artificially activated by treatment with its activators, complex effects may be expected in different organs. Although activation of AMPK has a number of potentially beneficial anti-atherosclerotic effects, including reducing adhesion of inflammatory cells to the endothelium, preventing lipid accumulation in blood vessel walls, and stimulating cellular antioxidant defences and enzymes responsible for NO formation, data from the present study suggest that prolonged activation of AMPK in endothelium may elicit adverse effects on liver functions under obese conditions. A previous study also found that expression of constitutively active AMPK α2 led to fatty liver due to a switch from glucose production to lipid generation (Foretz *et al.*, 2005). Collectively, these lines of evidence indicate that while AMPK activation may have beneficial potential in the treatment of cardiometabolic abnormalities, it needs to be controlled temporally and spatially in order to prevent unwanted pro-inflammatory effects.

The present study also suggests that endothelial dysfunction represents a common aetiology for both cardiovascular and non-alcoholic fatty liver diseases. Hyperactivation of AMPK signalling promotes senescence in endothelial cells and enhances the production of pro-inflammatory cytokines and lipid metabolites (Zu *et al.*, 2010; Wang *et al.*, 2011; Bai *et al.*, 2012), in turn, mediating systemic inflammation in blood vessels and organs, such as liver. In addition, the gene expression levels of EL and LDLR were decreased in endothelial cells of EC-AMPK mice, which contributed to the elevated lipid levels in circulation and the abnormal lipid metabolism in liver. The above two arms of defects are largely blocked by chronic treatment with COX-2 inhibitors, confirming that endothelial dysfunction represents a primary cause of metabolic syndrome in EC-AMPK mice. Nevertheless, further investigations are needed to uncover the mechanisms underlying the augmented plasma glucose levels and systolic BPs.

Acknowledgements

This work was supported, in part, by grants from Seeding Funds for Basic Research of the University of Hong Kong, and Research Grant Council (HKU781311M and HKU780410M) under the University Grants Committee, and Health and Medical Research Fund (11121651), HKSAR.

Conflict of interest

None declared.

References

Bai B, Liang Y, Xu C, Lee MY, Xu A, Wu D *et al.* (2012). Cyclin-dependent kinase 5-mediated hyperphosphorylation of sirtuin-1 contributes to the development of endothelial senescence and atherosclerosis. Circulation 126: 729–740.

Breinig M, Schirmacher P, Kern MA (2007). Cyclooxygenase-2 (COX-2)-a therapeutic target in liver cancer? Curr Pharm Des 13: 3305–3315.

Brkic L, Riederer M, Graier WF, Malli R, Frank S (2012). Acyl chain-dependent effect of lysophosphatidylcholine on cyclooxygenase (COX)-2 expression in endothelial cells. Atherosclerosis 224: 348–354.

Cannon CP, Cannon PJ (2012). COX-2 inhibitors and cardiovascular risk. Science 336: 1386–1387.

Cao J, Sodhi K, Puri N, Monu SR, Rezzani R, Abraham NG (2011). High fat diet enhances cardiac abnormalities in SHR rats: protective role of heme oxygenase-adiponectin axis. Diabetol Metab Syndr 3: 37.

Carling D, Thornton C, Woods A, Sanders MJ (2012). AMP-activated protein kinase: new regulation, new roles? Biochem J 445: 11–27.

Chang MY, Ho FM, Wang JS, Kang HC, Chang Y, Ye ZX *et al.* (2010). AICAR induces cyclooxygenase-2 expression through AMP-activated protein kinase-transforming growth factor-beta-activated kinase 1-p38 mitogen-activated protein kinase signaling pathway. Biochem Pharmacol 80: 1210–1220.

Chen L, Jiao ZH, Zheng LS, Zhang YY, Xie ST, Wang ZX *et al.* (2009). Structural insight into the autoinhibition mechanism of AMP-activated protein kinase. Nature 459: 1146–1149.

Davis BJ, Xie Z, Viollet B, Zou MH (2006). Activation of the AMP-activated kinase by antidiabetes drug metformin stimulates nitric oxide synthesis *in vivo* by promoting the association of heat shock protein 90 and endothelial nitric oxide synthase. Diabetes 55: 496–505.

Demirel U, Yalniz M, Aygun C, Orhan C, Tuzcu M, Sahin K *et al.* (2012). Allopurinol ameliorates thioacetamide-induced acute liver failure by regulating cellular redox-sensitive transcription factors in rats. Inflammation 35: 1549–1557.

Dey A, Williams RS, Pollock DM, Stepp DW, Newman JW, Hammock BD *et al.* (2004). Altered kidney CYP2C and cyclooxygenase-2 levels are associated with obesity-related albuminuria. Obes Res 12: 1278–1289.

Di Francesco L, Totani L, Dovizio M, Piccoli A, Di Francesco A, Salvatore T *et al.* (2009). Induction of prostacyclin by steady laminar shear stress suppresses tumor necrosis factor-alpha biosynthesis via heme oxygenase-1 in human endothelial cells. Circ Res 104: 506–513.

Eligini S, Habib A, Lebret M, Creminon C, Levy-Toledano S, Maclouf J (2001). Induction of cyclo-oxygenase-2 in human endothelial cells by SIN-1 in the absence of prostaglandin production. Br J Pharmacol 133: 1163–1171.

Eligini S, Barbieri SS, Cavalca V, Camera M, Brambilla M, De Franceschi M *et al.* (2005). Diversity and similarity in signaling events leading to rapid Cox-2 induction by tumor necrosis factor-alpha and phorbol ester in human endothelial cells. Cardiovasc Res 65: 683–693.

Eligini S, Arenaz I, Barbieri SS, Faleri ML, Crisci M, Tremoli E *et al.* (2009). Cyclooxygenase-2 mediates hydrogen peroxide-induced wound repair in human endothelial cells. Free Radic Biol Med 46: 1428–1436.

Ewart MA, Kennedy S (2011). AMPK and vasculoprotection. Pharmacol Ther 131: 242–253.

Faour WH, Gomi K, Kennedy CR (2008). PGE(2) induces COX-2 expression in podocytes via the EP(4) receptor through a PKA-independent mechanism. Cell Signal 20: 2156–2164.

Feng L, Xia Y, Garcia GE, Hwang D, Wilson CB (1995). Involvement of reactive oxygen intermediates in cyclooxygenase-2 expression induced by interleukin-1, tumor necrosis factor-alpha, and lipopolysaccharide. J Clin Invest 95: 1669–1675.

Fisslthaler B, Fleming I (2009). Activation and signaling by the AMP-activated protein kinase in endothelial cells. Circ Res 105: 114–127.

Foretz M, Ancellin N, Andreelli F, Saintillan Y, Grondin P, Kahn A *et al.* (2005). Short-term overexpression of a constitutively active form of AMP-activated protein kinase in the liver leads to mild hypoglycemia and fatty liver. Diabetes 54: 1331–1339.

Giannitrapani L, Ingrao S, Soresi M, Florena AM, La Spada E, Sandonato L *et al.* (2009). Cyclooxygenase-2 expression in chronic liver diseases and hepatocellular carcinoma: an immunohistochemical study. Ann N Y Acad Sci 1155: 293–299.

Goirand F, Solar M, Athea Y, Viollet B, Mateo P, Fortin D *et al.* (2007). Activation of AMP kinase alpha1 subunit induces aortic vasorelaxation in mice. J Physiol 581 (Pt 3): 1163–1171.

Hardie DG (2011). AMP-activated protein kinase: an energy sensor that regulates all aspects of cell function. Genes Dev 25: 1895–1908.

Hardie DG, Ross FA, Hawley SA (2012). AMPK: a nutrient and energy sensor that maintains energy homeostasis. Nat Rev Mol Cell Biol 13: 251–262.

Hawley SA, Fullerton MD, Ross FA, Schertzer JD, Chevtzoff C, Walker KJ *et al.* (2012). The ancient drug salicylate directly activates AMP-activated protein kinase. Science 336: 918–922.

Henry M, Davidson L, Cohen Z, McDonagh PF, Nolan PE, Ritter LS (2009). Whole blood aggregation, coagulation, and markers of platelet activation in diet-induced diabetic C57BL/6J mice. Diabetes Res Clin Pract 84: 11–18.

Hou CH, Tan TW, Tang CH (2008). AMP-activated protein kinase is involved in COX-2 expression in response to ultrasound in cultured osteoblasts. Cell Signal 20: 978–988.

Hsieh PS, Jin JS, Chiang CF, Chan PC, Chen CH, Shih KC (2009). COX-2-mediated inflammation in fat is crucial for obesity-linked insulin resistance and fatty liver. Obesity (Silver Spring) 17: 1150–1157.

Kahn BB, Alquier T, Carling D, Hardie DG (2005). AMP-activated protein kinase: ancient energy gauge provides clues to modern understanding of metabolism. Cell Metab 1: 15–25.

Kilkenny C, Browne W, Cuthill IC, Emerson M, Altman DG (2010). Animal research: Reporting *in vivo* experiments: the ARRIVE guidelines. Br J Pharmacol 160: 1577–1579.

Kim SY, Jeong S, Jung E, Baik KH, Chang MH, Kim SA *et al.* (2012). AMP-activated protein kinase-alpha1 as an activating kinase of TGF-beta-activated kinase 1 has a key role in inflammatory signals. Cell Death Dis 3: e357.

Kwon SH, Jeong SW, Jang JY, Lee JE, Lee SH, Kim SG *et al.* (2012). Cyclooxygenase-2 and vascular endothelial growth factor in chronic hepatitis, cirrhosis and hepatocellular carcinoma. Clin Mol Hepatol 18: 287–294.

Law IK, Xu A, Lam KS, Berger T, Mak TW, Vanhoutte PM *et al.* (2010). Lipocalin-2 deficiency attenuates insulin resistance associated with aging and obesity. Diabetes 59: 872–882.

Lee JY, Choi AY, Oh YT, Choe W, Yeo EJ, Ha J *et al.* (2012). AMP-activated protein kinase mediates T cell activation-induced expression of FasL and COX-2 via protein kinase C theta-dependent pathway in human Jurkat T leukemia cells. Cell Signal 24: 1195–1207.

Li FY, Lam KS, Tse HF, Chen C, Wang Y, Vanhoutte PM *et al.* (2012). Endothelium-selective activation of AMP-activated protein kinase prevents diabetes mellitus-induced impairment in vascular function and reendothelialization via induction of heme oxygenase-1 in mice. Circulation 126: 1267–1277.

Liu C, Liang B, Wang Q, Wu J, Zou MH (2010). Activation of AMP-activated protein kinase alpha1 alleviates endothelial cell apoptosis by increasing the expression of anti-apoptotic proteins Bcl-2 and survivin. J Biol Chem 285: 15346–15355.

Liu JT, Song E, Xu A, Berger T, Mak TW, Tse HF *et al.* (2012). Lipocalin-2 deficiency prevents endothelial dysfunction associated with dietary obesity: role of cytochrome P450 2C inhibition. Br J Pharmacol 165: 520–531.

McGrath J, Drummond G, McLachlan E, Kilkenny C, Wainwright C (2010). Guidelines for reporting experiments involving animals: the ARRIVE guidelines. Br J Pharmacol 160: 1573–1576.

Miyashita M, Ito T, Sakaki M, Kajiwara A, Nozawa H, Hiroishi K *et al.* (2012). Genetic polymorphism in cyclooxygenase-2 promoter affects hepatic inflammation and fibrosis in patients with chronic hepatitis C. J Viral Hepat 19: 608–614.

Paik YH, Kim JK, Lee JI, Kang SH, Kim DY, An SH *et al.* (2009). Celecoxib induces hepatic stellate cell apoptosis through inhibition of Akt activation and suppresses hepatic fibrosis in rats. Gut 58: 1517–1527.

Planaguma A, Claria J, Miquel R, Lopez-Parra M, Titos E, Masferrer JL *et al.* (2005). The selective cyclooxygenase-2 inhibitor SC-236 reduces liver fibrosis by mechanisms involving non-parenchymal cell apoptosis and PPARgamma activation. FASEB J 19: 1120–1122.

Sanchez A, Contreras C, Martinez P, Villalba N, Benedito S, Garcia-Sacristan A *et al.* (2010). Enhanced cyclooxygenase 2-mediated vasorelaxation in coronary arteries from insulin-resistant obese Zucker rats. Atherosclerosis 213: 392–399.

Santilli F, Vazzana N, Liani R, Guagnano MT, Davi G (2012). Platelet activation in obesity and metabolic syndrome. Obes Rev 13: 27–42.

Stein SC, Woods A, Jones NA, Davison MD, Carling D (2000). The regulation of AMP-activated protein kinase by phosphorylation. Biochem J 345 (Pt 3): 437–443.

Szerafin T, Erdei N, Fulop T, Pasztor ET, Edes I, Koller A *et al.* (2006). Increased cyclooxygenase-2 expression and prostaglandin-mediated dilation in coronary arterioles of patients with diabetes mellitus. Circ Res 99: e12–e17.

Tong X, Peng H, Liu D, Ji L, Niu C, Ren J *et al.* (2013). High-density lipoprotein of patients with type 2 diabetes mellitus upregulates cyclooxgenase-2 expression and prostacyclin I-2 release in endothelial cells: relationship with HDL-associated sphingosine-1-phosphate. Cardiovasc Diabetol 12: 27.

Tu CT, Guo JS, Wang M, Wang JY (2007). Antifibrotic activity of rofecoxib in vivo is associated with reduced portal hypertension in rats with carbon tetrachloride-induced liver injury. J Gastroenterol Hepatol 22: 877–884.

Wang S, Zhang M, Liang B, Xu J, Xie Z, Liu C *et al.* (2010). AMPKalpha2 deletion causes aberrant expression and activation of NAD(P)H oxidase and consequent endothelial dysfunction *in vivo*: role of 26S proteasomes. Circ Res 106: 1117–1128.

Wang Y, Liang Y, Vanhoutte PM (2011). SIRT1 and AMPK in regulating mammalian senescence: a critical review and a working model. FEBS Lett 585: 986–994.

Woods A, Johnstone SR, Dickerson K, Leiper FC, Fryer LG, Neumann D *et al*. (2003). LKB1 is the upstream kinase in the AMP-activated protein kinase cascade. Curr Biol 13: 2004–2008.

Yu Y, Ricciotti E, Scalia R, Tang SY, Grant G, Yu Z *et al*. (2012). Vascular COX-2 modulates blood pressure and thrombosis in mice. Sci Transl Med 4: 132ra154.

Zhang J, Bowden GT (2008). UVB irradiation regulates Cox-2 mRNA stability through AMPK and HuR in human keratinocytes. Mol Carcinog 47: 974–983.

Zhou M, Xu A, Lam KS, Tam PK, Che CM, Chan L *et al*. (2010). Rosiglitazone promotes fatty acyl CoA accumulation and excessive glycogen storage in livers of mice without adiponectin. J Hepatol 53: 1108–1116.

Zhou M, Xu A, Tam PK, Lam KS, Huang B, Liang Y *et al*. (2012). Upregulation of UCP2 by adiponectin: the involvement of mitochondrial superoxide and hnRNP K. PloS One 7: e32349.

Zu Y, Liu L, Lee MY, Xu C, Liang Y, Man RY *et al*. (2010). SIRT1 promotes proliferation and prevents senescence through targeting LKB1 in primary porcine aortic endothelial cells. Circ Res 106: 1384–1393.

Supporting Information

Additional Supporting Information may be found in the online version of this article at the publisher's web-site:

http://dx.doi.org/10.1111/bph.12482

Figure S1 Impaired glucose tolerance in EC-AMPK mice given a high fat diet. The ipGTT was performed in wild-type and EC-AMPK mice fed with the high fat diet for 16 weeks. Results are presented as percentage changes of blood glucose levels against time zero (A). The areas under the curve (AUC) were calculated and are presented as means ± SEM (B). *P < 0.05, compared with wild-type mice (n = 5).

Figure S2 Increased AMPK activity in non-parenchymal cells isolated from liver tissues of EC-AMPK mice. Liver cell fractionation was performed as described in the Methods section. Samples derived from non-parenchymal cells were subjected to RT-PCR (A) and AMPK activity (B) analysis for monitoring the CA-AMPK transgene expression. The elevated AMPK activity was also confirmed by probing the phosphorylation levels of acetyl-CoA carboxylase (ACC) (C), a downstream substrate of AMPK. *P < 0.05, compared with wild-type mice (n = 5).

Figure S3 Decreased EL and LDLR expression in tissues of EC-AMPK mice. After 16 weeks of high fat diet, the aortae and liver tissues were collected from wild-type and EC-AMPK mice. Quantitative RT-PCR was performed to evaluate the gene expression of EL and LDLR. *P < 0.05 versus wild-type mice group (n = 3–5).

Figure S4 COX-2 selective inhibitor treatment did not change the AMPK activity in the aorta. Wild-type and EC-AMPK mice given a high fat diet were treated with vehicle or celecoxib (50 mg·kg^{-1}·day^{-1}) for 4 weeks. At the end of treatment, aorta tissues were collected and subjected to the measurement of AMPK activity. Relative comparisons were calculated against samples from wild-type mice treated with vehicle. *P < 0.05 versus wild-type mice treated with vehicle (n = 3–5).

Figure S5 Treatment with COX-2 selective inhibitors did not affect the blood pressure, blood clotting capacity and tissue TxB_2 concentrations. (A) After 4 weeks of treatment with vehicle or celecoxib, systolic (left panel) and diastolic (right panel) blood pressures were measured in wild-type mice given a high fat diet. (B) Wild-type (left panel) and EC-AMPK (right panel) mice under high-fat diet were treated with vehicle, celecoxib (50 mg·kg^{-1}·day^{-1}) or nimesulide (25 mg·kg^{-1}·day^{-1}) for a period of 4 weeks. At the end of treatment, the blood clotting capacity of the mice was evaluated. (C) The aortae and liver tissues were collected from mice treated as in panel (B) and TxB_2 concentrations were measured. Relative changes were calculated against samples from mice treated with vehicle (n = 3–5).

Table S1 List of primers used for quantitative PCR analysis.